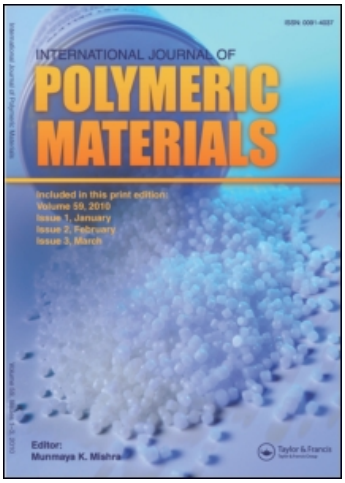

International Journal of Polymeric Materials
Publication details, including instructions for authors and subscription information:
http://www.informaworld.com/smpp/title~content=t713647664

The Electro-Optical Effect in Poled Side Chain Polymers

C. P. J. M. van der Vorst[a]; M. van Rheede[a]; C. J. M. van Weerdenburg[a]
[a] Akzo Research Laboratories Arnhem Applied Physics Department, Corporate Research, Arnhem, The Netherlands

To cite this Article van der Vorst, C. P. J. M. , van Rheede, M. and van Weerdenburg, C. J. M.(1993) 'The Electro-Optical Effect in Poled Side Chain Polymers', International Journal of Polymeric Materials, 22: 1, 113 — 125
To link to this Article: DOI: 10.1080/00914039308012065
URL: http://dx.doi.org/10.1080/00914039308012065

Intern. J. Polymeric Mater., 1993, Vol. 22, pp. 113–125
Reprints available directly from the publisher
Photocopying permitted by license only

Printed in Malaysia

The Electro-Optical Effect in Poled Side Chain Polymers

C. P. J. M. VAN DER VORST, M. VAN RHEEDE, and C. J. M. VAN WEERDENBURG

Akzo Research Laboratories Arnhem Applied Physics Department, Corporate Research PO Box 9300, 6800 SB Arnhem, The Netherlands

The linear electro-optical effect has been studied in test samples of two different nonlinear optical polymers—with T_g of 140°C and 175°C, respectively—*during* and *after poling*. The electro-optical coefficients were measured between crossed polarizers ($r_{33} - r_{13}$) and using the test samples as Fabry–Perot interferometers (r_{13}). The field strength dependence of the coefficients has been measured during poling of the polymer with $T_g = 140$°C, and compared with theory. Also, the ratio r_{33}/r_{13} has been investigated. A quasi-instantaneous loss of the field-induced electro-optical activity is observed when the poling field is switched off at ambient temperature after poling in the vicinity of T_g. The influence of an annealing step on the relaxation behavior is discussed. Results of relaxation experiments in the two polymers performed at several constant temperatures are presented.

KEY WORDS Electro-optics, Pockels effect, poling, relaxation, annealing, side chain polymer.

1. INTRODUCTION

Poled side chain polymers, with acceptor-donor substituted conjugated π electron systems (AπD) incorporated in the side chains, are promising materials for manufacturing electro-optical (EO) devices. Such devices—switches and modulators—can be used in future telecommunication networks.[1–5] The switching capabilities are based on the linear EO effect in the poled polymers, which is a consequence of their second-order non-linear optical (NLO) properties. These macroscopic properties are based, in turn, on the corresponding molecular second-order nonlinear optical property (hyperpolarizability) of the AπD entities.

For second-order nonlinearity, no centrosymmetry is necessary. In the materials studied, this requirement holds both on a molecular and on a macroscopic level. The requirement of noncentrosymmetry on a molecular level is evidently fulfilled in the AπD molecules. To induce second-order nonlinearity on a macroscopic level, the orientational distribution function of the AπD groups has to become noncentrosymmetrical. This is accomplished by aligning the permanent dipole moments of the AπD molecules with a strong electric field at or near the polymer's glass transition temperature T_g ("poling"), followed by "freezing-in" the induced orientational order by cooling to temperatures far below T_g. When the poling field is switched off, the poled polymer is not in thermodynamical equilibrium. Hence, the poled state is inherently unstable. This is acceptable as long as relaxation of orientational order remains within user-defined boundaries, with respect to time and temperature. Present day NLO polymers do not fulfill the stability requirements yet. Plausible strategies which

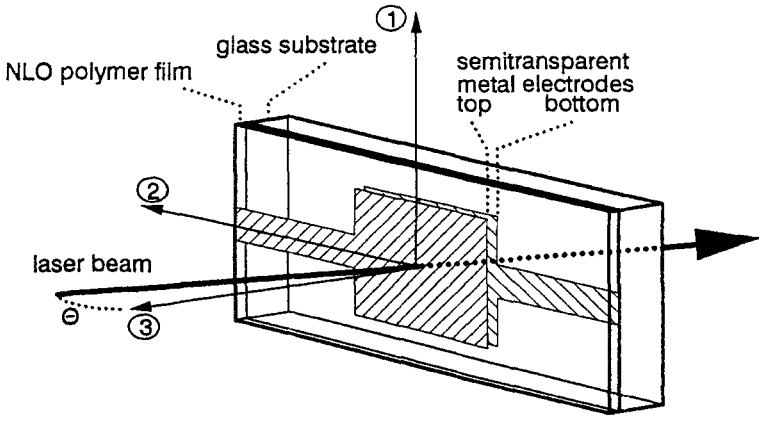

FIGURE 1 Polymer test sample on rectangular glass substrate. Unit vectors are labeled 1, 2, and 3.

will improve the thermal stability are cross-linking and T_g-increase.

By coupling hyperpolarizable moieties of 4-dimethylamino-4′-nitrostilbene (DANS) to a suitable backbone polymers with moderate thermal stability of poling-induced orientational order have been obtained at Akzo. Devices based on these DANS substituted polymers show good performance. Large Pockels coefficients up to 34 pm/V have been realized in polymeric waveguide devices. Mach–Zehnder interferometers with switching voltages of 5 V, optical attenuations below 1 dB/cm and a frequency response up to at least 20 GHz are possible.[4–7] Here, results of poling and relaxation experiments in test samples of two NLO polymers with values of $T_g = 140°C$ and 175°C are presented.

2. MEASURING METHODS

For the investigation of poling and relaxation in NLO polymers we use simple test samples consisting of a single NLO polymer layer sandwiched between a pair of plane parallel, semitransparent metal electrodes.[8–9] They can be measured in *transmission or reflection.* Multilayer packets like in waveguiding devices (NLO core layer plus buffer or cladding layers) can be studied using the same technique(s). The substrates for the test samples are either glass microscope slides or silicon wafers. Figure 1 shows a single layer sample on a glass slide. The optical wavelength used for all measurements on test samples is 633 nm (HeNe-laser).

For EO measurements in the above mentioned test samples, a number of measuring methods are available at our laboratories. These methods differ in one or more of the following respects (which are sometimes linked):

(i) the *propagation mode* of the experiment: transmission (for glass substrates) or reflection (silicon substrates);

(ii) the *conversion mechanism* which converts the electro-optic modulation of the refractive index (Pockels effect) into a measurable modulation of a light intensity: interference (Mach–Zehnder interferometer, Fabry–Perot interferometer) or polarization selective absorption (crossed polarizer);

(iii) the *physical quantity or quantities* obtained from the experiment.

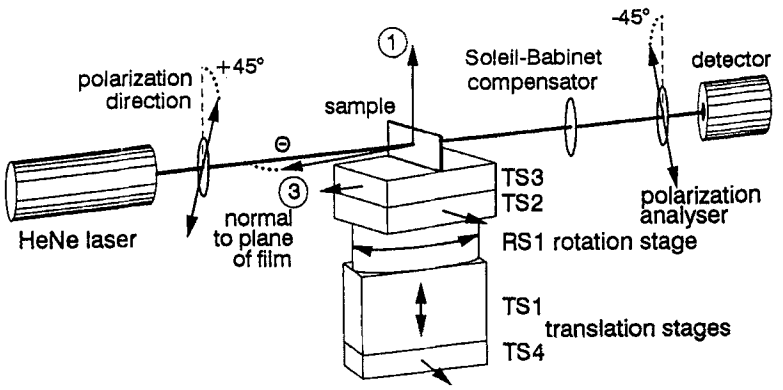

FIGURE 2 Transmission setup for crossed polarizers and Fabry–Perot measurements in the polymer test sample of Figure 1. As shown, the setup is in the crossed polarizers mode of operation.

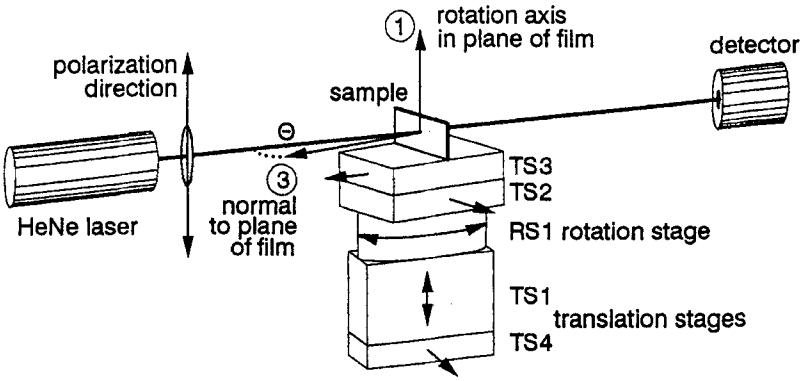

FIGURE 3 Transmission setup in the Fabry–Perot mode of operation.

We use the angle-tuned Fabry–Perot interferometric technique[9,10] for measurement of the Pockels coefficient r_{13} and of the layer thickness d, whereas the difference of Pockels coefficients $(r_{33} - r_{13})$ is determined between crossed polarizers.[8,9] For the measurement of r_{13} the laser beam is polarized parallel to the rotation axis of the sample (s-polarization); for the measurement of $(r_{33} - r_{13})$ the polarization direction is at 45° with respect to the rotation axis.

The experimental quantities d, r_{13}, and $(r_{33} - r_{13})$ can be determined at nearly the same sample spot, using common setups for the Fabry–Perot (FP) and crossed polarizers (CP) experiments.[9] Different versions of such common setups are used for the transmission and the reflection experiments. Figure 2 shows the test sample on glass in the transmission setup. The CP mode of operation is shown. The FP mode of operation is presented in Figure 3. Combination of the results of FP and CP experiments at the same spot gives the values of r_{13} and r_{33} separately, and of their ratio r_{33}/r_{13}. The coefficient r_{13} can also be measured in transmission using a Mach–Zehnder interferometer,[8,11] but this needs placement of the sample in a different setup.

For the calculation of the layer thickness d from an angular intensity scan $I(\theta)$ (I is the intensity of the transmitted or reflected beam, θ is the angle of incidence), a simple

procedure is used which needs the value of the refractive index n as a known input parameter:

(i) the angles θ_m are determined at which the transmission is maximal or the reflection minimal (m is peak number),

(ii) the function $(1 - \sin^2\theta_m/n^2)^{1/2}$ is plotted versus m,

(iii) the plot is fitted with a straight line with slope $\lambda/2dn$ (λ is the wavelength),

(iv) the layer thickness is calculated from the slope.

In near future, we hope to be able to determine layer thicknesses, anisotropic refractive indices and absorption coefficients, as well as EO coefficients from FP experiments with s- and p-polarization. This needs automation of the measuring setup and more exact, but more elaborate, numerical data evaluation.

Our earlier EO experiments were in transmission using glass microscope slides, transparent for the HeNe-wavelength, as the substrate. Nowadays, we prefer silicon wafers as the substrate, as these have a number of advantages over the glass microscope slides. Since doped silicon is semiconducting the metal lower electrode can, in principle, be omitted. More important is that the uniformity of the spincoated polymer layers is better than on microscope slides. Unfortunately, silicon is not transparent for 633 nm or any other visible wavelength. Since we appreciate working with visible light (despite resonance-enhancement of r), we have built a *reflection* setup for measurements in NLO test samples on silicon, analogous to the *transmission* measurements in samples on glass.

The sample holders in the reflection and transmission setups are temperature-controlled to allow measurements at elevated temperatures. In the experimental setups, the samples can be poled and annealed *in situ*, applying a DC voltage to the plane parallel electrodes. Measurements of the Pockels coefficient are possible between ambient temperature and 250°C. Such measurements can be performed as a function of time at a constant temperature both in the poled samples (relaxation experiments) or during poling. In the relaxation experiments only an AC modulation voltage is applied. Because of the small optical path length used (a few microns), the EO intensity modulation is generally small and phase sensitive techniques have to be applied for detection. In the experiments during poling, a superposition of a DC and an AC voltage is used. The DC component is used for measuring the EO induced coefficients, the AC part is for measuring the DC induced coefficients, DC induced Pockels effect having been previously measured.[2,9]

3. SAMPLE PREPARATION

Test samples were prepared of DANS containing side chain polymer[9] with $T_g = 140$°C. This value is the T_g onset as determined from differential scanning calorimetry (DSC) measurements. The refractive index has been obtained from prism coupling experiments: n is 1.69 at 633 nm and 1.62 at 1320 nm. Test samples were also prepared from a new polymer with $T_g = 175$°C and a refractive index of 1.70 (at 633 nm), containing DANS-like active groups. The test samples consist of a polymer layer between plane parallel, semitransparent metal electrodes on a glass or silicon substrate. The glass substrates are 26×76 mm^2 microscope slides; the silicon substrates are round wafers of 3 inches diameter. Prior to the first metallization step, the substrates were cleaned *in situ* in the evaporation chamber with a glow discharge. The lower electrodes on glass usually are of silver with a thickness of about 25 nm (transmission 10%) and an area of 20×20 mm^2.

The lower electrodes on silicon (if applied) cover the whole wafer and consist of a 10 nm thin chromium adherence layer followed by a 100 nm thick gold layer. Polymer films were prepared by spincoating from a filtered polymer solution in cyclopentanone. After spinning, the samples were heated for a few hours on a hot stage slightly above T_g, in order to remove traces of solvent and relieve solvent stress. Finally, the semitransparent top electrode was evaporated. The top electrode on glass is similar to the lower one. The top electrode on a silicon wafer consists of a 10 nm thin gold layer, 62 mm in diameter. Polymer layer thicknesses were measured by a Fabry–Perot interferometer at the measure spot of the EO experiments. The obtained thicknesses were in agreement with profilometric measurements (step profile over scratch in polymer layer) performed after the EO experiments.

4. RESULTS AND DISCUSSION

4.1. DANS polymer with $T_g = 140°C$

4.1.1. Dependence of EO coefficients on poling field strength

The dependence of the EO coefficients r_{13} and r_{33} on the poling field strength has been investigated in the DANS polymer with $T_g = 140°C$ for field strength up to 110 V/μm.

For the poling of isotropic non-liquid crystalline media the isotropic model[12,13] predicts a linear dependence of the relevant order parameters on the field strength for values of the relative dipole energy $a = \mu E/kT$ up to a value of 1–2, followed by saturation for much higher values of a. Here μ is the permanent dipole moment of the AπD group, E is the (local) poling field, T is the poling temperature and k is Boltzmann's constant. The extended Maier–Saupe model[2,14] predicts the possibility of a region with superproportional behavior between the linear and the subproportional regions depending on the input parameters of the model. However, one of these, the value of the zero-field clearing temperature T_c, is difficult to obtain in non-liquid crystalline polymers, where T_c corresponds to a virtual transition ($T_c > T_g$). It is therefore difficult to tell for actual materials whether the model does or does not predict a superlinear region. What remains is experimental verification. So far, no cases of superproportional poling behavior have been reported in the literature, except by Stamatoff[15] (see Figure 1 of this Reference).

We have checked the dependence of the EO coefficients *during poling* at 130–135°C, since theoretical predictions are expected to hold best in this situation. No additional assumption is necessary, such as perfect freezing-in of field-induced order.[2]

During FP and CP experiments using samples on glass and silicon substrates, the EO intensity modulation (output of lock-in amplifier) was plotted versus the DC poling voltage applied to the electrodes. At least 15 experiments were performed using 13 samples, with layer thicknesses in the range 3.8–4.5 μm and maximum DC voltages in the range 220–460 V. The highest values of the poling field strengths attained were slightly in excess of 100 V/μm. Approaching the highest voltages in each experiment many temporary breakdowns occurred at weak spots in the samples. The first dielectric breakdown was "self-healing", viz. temporary short-circuiting was removed by partial destruction of the sample at the weak spots. Later breakdowns were more destructive and most samples did not survive the poling tests.

Prior to the experiments, the angle of incidence was set at an optimum value.[9] For the FP experiments, this is at an angle with the steepest slope $dI/d\theta$, where the EO intensity

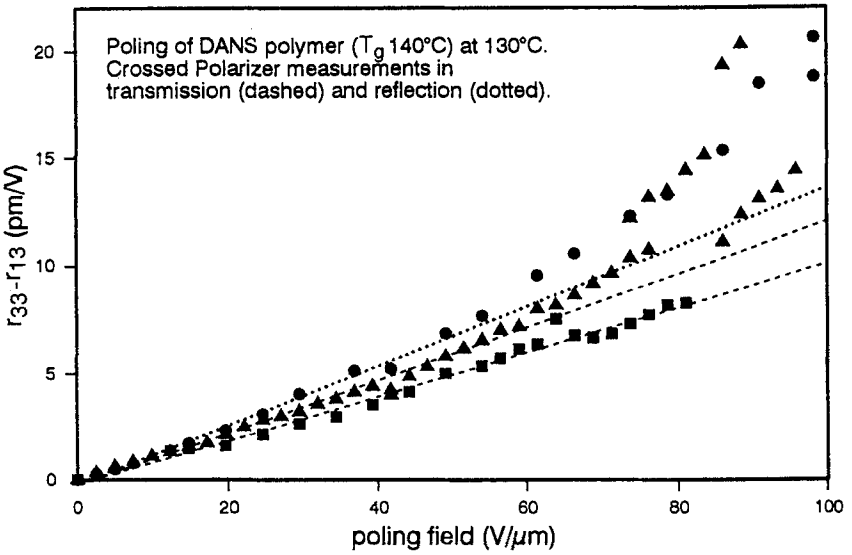

FIGURE 4 Dependence of EO coefficients on poling field strength.

modulation is also the largest. For a CP experiment this is at an extremum of $I(\theta)$, where interferometric intensity modulation is reduced and the optical path length is enhanced by a factor f.[8,9] The CP intensity modulation was maximized with a Soleil–Babinet compensator. It was found from the first tests that the initial optical alignments were not maintained during the voltage increase, as the peaks in $I(\theta)$ move. Periodic readjustments in angle (FP and CP) and total retardation (with compensator in CP measurements) were necessary. If readjustments were not applied, this easily led to false results (FP: apparently sublinear behavior; CP: apparently strong superproportional behavior). For precise measurements the AC modulation voltage was measured at the electrodes near the measure spot. The enhancement factor f was also measured thereafter. A compromise had to be found between fast measurements with few intermediate readjustments and/or readings and a low chance for electrical deterioration on the one hand, and more time-consuming, more accurate measurements with a higher chance for electrical deterioration and a lower maximum poling field strength on the other hand.

From the experiments it was found that $(r_{33} - r_{13})$ is a linear function of the poling field strength up to values of 50–80 V/μm. For higher field strengths, however, we do observe indications of superproportional behavior. Figure 4 shows the results in three samples, one on silicon, two on glass. In one of the samples on glass, breakdown occurred at the measure spot slightly below 80 V/μm. Measurements were continued at two other sample spots (Figure 4). The dependence of r_{13} on the poling field strength may be linear, perhaps slightly superproportional, but to a much lesser extent than is the case in $(r_{33} - r_{13})$.

4.1.2. Magnitude of EO coefficients

The average values of the EO coefficients obtained during poling with a poling field strength of 50 V/μm are $(r_{33} - r_{13})_{av} = 6.49 \pm 0.73$ pm/V (4 experiments) and $(r_{13})_{av} = 3.18 \pm 0.69$ pm/V (4 experiments). As the field strength of 50 V/μm is still in the linear

regime, these experimental values can be compared with the theoretical predictions from the isotropic model for poling. With an estimate for the product $\mu\beta$ for DANS of 6×10^{-45} esu, a number density of 1.26 nm^{-3}, a poling temperature of 403 K and assuming simple Lorentz local field factors ($(n^2+2)/3$ with isotropic $n = 1.69$) to convert applied fields into local field ($\times 4$), one calculates a theoretical value for $r_{33} - r_{13} = 2r_{13} = 20$ pm/V. This theoretical estimate is extremely rough due to uncertainty in the input parameters of the model, especially the hyperpolarizability (resonance enhanced) and the complexity of the local field problem. The discrepancy between experiment and theory, which amounts to a factor 3, is due in part to imperfect rotatability of the side chains. The discrepancy between experiment and theory becomes even higher if the measurements are performed *after* poling instead of *during* poling, because of non-ideal freezing-in of orientational order.[2,9] See also Section 4.2.1.

4.1.3. Ratio of EO coefficients

Combination of the experimental values of $(r_{33} - r_{13})_{av}$ and $(r_{13})_{av}$ gives the ratio: $(r_{33})_{av}/(r_{13})_{av} = 3.0 \pm 0.7$. The inaccuracy is significant since only 4 CP and 4 FP experiments were used for the calculation, each experiment being performed in a different sample at one sample spot only. For a more accurate determination of the ratio, more experiments are needed, preferable CP and FP measurements should be performed at different common sample spots. Such measurements have been made at ambient temperature in a poled sample (30 spots) of the DANS polymer.[9] A ratio of $r_{33}/r_{13} = 3.0 \pm 0.2$ was then found which appeared to be in good agreement with the ratio of 3, which is predicted by the isotropic poling model for small birefringence.

Such good agreement is not generally obtained. At present, the ratio r_{33}/r_{13} is being investigated more accurately in several different NLO polymers. Measurements are performed with the poling field on and off. The first results indicate serious deviations from the theoretical value of 3 in some polymers. Most interestingly, the experimental values are *smaller* than 3, some even approaching the value of 2.

4.1.4. Influence of annealing on thermal stability

Poled samples of a NLO polymer are not in thermodynamical equilibrium and are inherently unstable. Not only is the field-induced orientational polarization unstable after the poling field has been switched off, but also the specific volume of the polymer is unstable (too high) below T_g. During the cooling step, following poling at T_g, the polymer is unable to reach the lower equilibrium value of the specific volume in the glass state at the lower temperatures, owing to the reduced motional freedom of the glassy state. The so called free volume—the difference between the non-equilibrium value and the equilibrium value of the specific volume— builds up during this cooling step. Both the free volume and the orientational polarization tend to vanish, making use of the small but non-zero motional freedom within this very free volume, which may entail remarks.

The first is that relaxation of the free volume, also called "physical ageing", is a self-limiting process. It proceeds increasingly slower because (i) the thermodynamic driving force, viz. the difference between the nonequilibrium and the equilibrium value of the specific volume (free volume), becomes smaller; and (ii) the decrease of the free volume restricts the motional freedom increasingly. Effect (i) by itself would give a decay that

is exponential in time, with a certain characteristic speed or relaxation frequency in the exponent. Effect (ii) means that this "characteristic" speed itself decreases in time.

The second remark is that relaxation of free volume and relaxation of orientational polarization are related, since both relaxation processes make use of the motional freedom within the free volume, and since generally (!) the two processes co-develop in time. This relationship is probably such that the physical ageing influences relaxation of orientational order, but not vice versa. In the first approximation, we can describe relaxation of the polar order as a process that proceeds exponentially in time with a characteristic speed or relaxation frequency α in the exponent: $r(t,T) = r(0,T)\exp[-\alpha(T)t]$. Because $\alpha(T)$ depends on temperature as well as on the dimension of the free volume—which decreases—it cannot be really constant in time. Indeed, we often observe a deviation from purely exponential decay ("purely" implying a constant α). Also, the relaxation frequency will depend on the thermal history of the sample. This possibly explains part of the poor reproducibility of the relaxation data, when care is not taken to perform the reproducible thermal pretreatment. As well as other workers[16] we tried to describe relaxation of the Pockels coefficient with a multi-exponential expression of time, with the total Pockels coefficient composed of as a sum of individual terms, each decaying exponentially with its own characteristic speed. However the physical justification for such a description seems doubtful. Although a bi-exponential expression often fits the time dependence of our relaxation measurements quite well, we were unable to find a meaningful description of the temperature dependence of the highest relaxation speed, viz. the one corresponding to the fast initial relaxation. This is contrary to the findings of Man and Yoon.[16]

The third remark is that relaxation of free volume and of orientational order are not necessarily co-developing processes in poled polymers. The processes can be decoupled (to some extent). By introducing an annealing step in the cooling period after poling at T_g, with the poling field still on, relaxation of the free volume can take place, whereas relaxation of orientational polarization cannot. Field-induced orientational order can even reach higher values below T_g (where poling still is possible), because of the $1/T$ dependence of poling.[12,13] Suitable annealing temperatures are within the range of some tens of degrees below T_g, where the poling process also still proceeds, but with a lower speed than at T_g.[9] This temperature range is also used for annealing (without field) of polymer casts in order to increase the shape stability. This advantage of annealing may also be of importance for EO devices. Another advantage is relaxation of thermal stress between polymer layers and the substrate to suppress crack-formation.

Samples of the DANS polymer annealed overnight at 117°C, following poling for 5 min at $T_g = 140$°C, showed increased thermal stability compared with non-annealed samples. Similar observations have been made by other groups.[16–18] The annealed samples showed a good single-exponential relaxation behavior at 117°C, whereas the non-annealed samples revealed fast initial relaxation ("bi-exponential behavior"). Some typical results are presented in Figure 5. After averaging over several experiments (only two are given in Figure 5) it was found that the final relaxation speed of the non-annealed samples approaches the value of the annealed samples. Annealing did not influence significantly the freezing-in efficiency factor η (defined in Section 4.2.1). In both annealed and non-annealed samples, η value obtained was about 0.66 ± 0.06. On the other hand, annealing did give a significantly higher initial value of the EO coefficient. The enhancement was by a factor of 1.15, which is larger than what was expected from the $1/T$ dependence

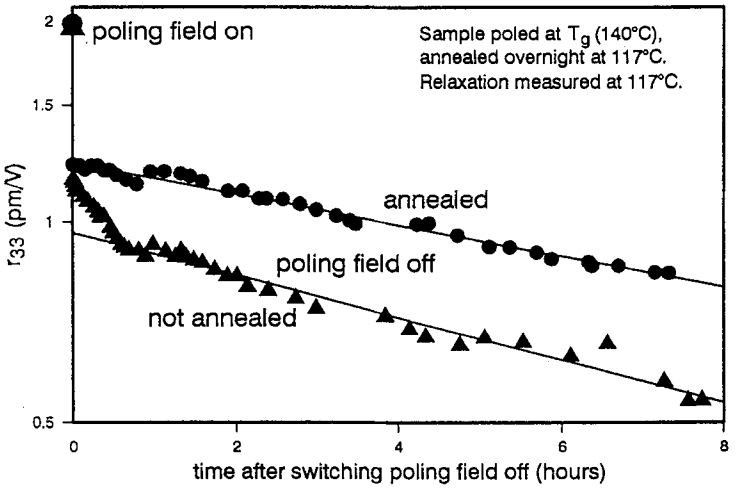

FIGURE 5 Influence of annealing on thermal stability.

(factor 1.06) alone. Possibly, the main poling step at 140°C was not long enough to reach equilibrium at 140°C, whereas equilibrium at 117°C was approached better in the annealing step (prolonged poling!).

4.1.5. Relaxation

Results of relaxation experiments performed in two batches of the DANS polymer at several constant temperatures in the range from 80°C to 135°C are shown in Figure 6. The EO coefficients were measured with FP interferometry and between crossed polarizers. The decay in time was fitted with a single-exponential expression of time t: $r(t,T) = r(0,T)\exp[-\alpha(T)t]$. This showed a good fit for the annealed samples. In the non-annealed samples the first data points showing fast initial relaxation were excluded from the fit. The remaining points could be fitted nicely with the single exponential expression. Relaxation frequencies $\alpha(T)$ obtained at different temperatures are shown in the Arrhenius plot of Figure 6 where $\ln[\alpha(T)]$ is plotted versus $1/T$. The straight lines fitting the results of the two polymer batches represent the Arrhenius curves $\alpha(T) = \alpha(\infty)\exp(-A/RT)$. Here R is the gas constant. The activation energy A can be calculated from the slope, and the preexponential factor $\alpha(\infty)$ from the intercept of the straight lines. Values for A and $\ln[\alpha(\infty)]$ obtained for the two polymer batches are given in Figure 6: A is 295 and 280 kJ/mol; $\ln[\alpha(\infty)]$ is 89 and 84, respectively (α in reciprocal hours). The difference between the two batches is not significant. All Arrhenius plots of several batches of the DANS polymer (including the two of Figure 6), obtained both from poling and relaxation measurements,[2,9,19] overlap each other and show activation energies in the vicinity of 300 kJ/mol.

4.2. Test polymer with $T_g = 175°C$

4.2.1. Initial poling experiments

Initial poling experiments in a test polymer with a DANS-like active group and $T_g = 175°C$ have been performed and compared with similar experiments in a DANS polymer with

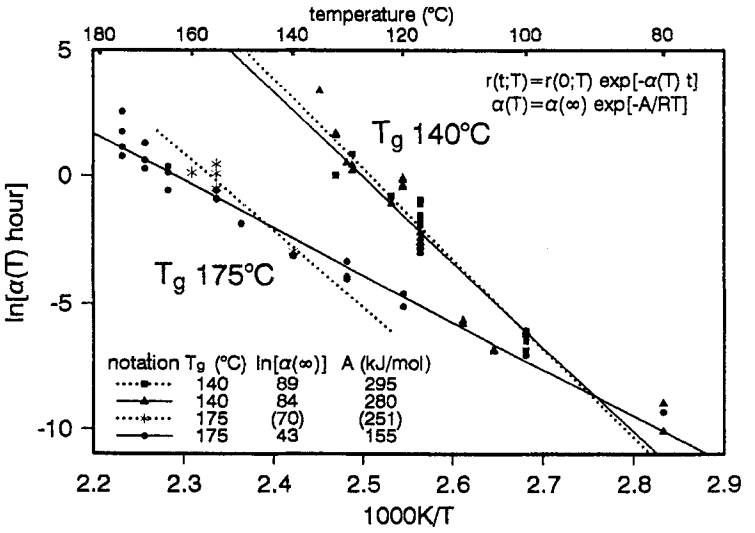

FIGURE 6 Arrhenius plot of thermal relaxation frequencies in polymers with $T_g = 140°C$ and $T_g = 175°C$ (2 batches of each polymer).

$T_g = 140°C$. The CD-induced Pockels effect technique was applied for the measurements during poling. The measurements were CP/FP measurements in transmission, with samples on glass being used.

It was observed in the test polymer that the Pockels effect can be induced by the DC field even at ambient temperature.[19] The response is quasi-instantaneous on the time scale of the experiments with phase sensitive detection (modulation frequency 325 Hz, lock-in time constant 0.3 s). The effect, however, is not lasting and disappears immediately as soon as the DC field is switched off again. Similar phenomena were observed in other NLO polymers as well, e.g. in the DANS polymer with $T_g = 140°C$.[2,9,20] See also Figure 5. Experiments at Lockheed revealed[20] that the quasi-instantaneous response develops and decays within 10 ms. Other observations are mentioned in Van der Vorst *et al.*[2] We attribute this effect to *reversible* orientation of donor-acceptor sidegroups within their polymer environment.[2] Part of this orientation may take place in the void volume ("free volume") surrounding the side chains, in which there is complete freedom to move without energetic changes. In a model, the side chains can be represented as rods "rattling" in a cage with hard walls. Even greater polarization is possible by *reversible* rearrangements within the environment, which accommodate the rotating sidegroup. This second contribution to polar order, in which elastic deformation energy is involved, can be represented in the above mentioned rattling rod model by soft (harmonic) walls. The orientational order disappears due to fast thermal relaxation and to elastic forces as soon as the poling field is switched off.

Polar order that can be "frozen in" arises when the elastic deformation energy is relieved during poling by plastic, irreversible rearrangements within the environment (rotation of cages). The *conversion* during poling of elastic environmental deformation into plastic deformation takes time which depends on temperature. The time-temperature characteristics of poling (as well as relaxation) have been studied in the DANS polymer with $T_g = 140°C$

in the temperature range 100°–140°C.[9]

The first signs of plastic behavior in the test polymer, observable within minutes, started at temperatures above 140–150°C. In addition to an instantaneous response after switching on the DC field, the Pockels effect also showed a *gradual* increase. When the DC field was switched off again, the response did not drop instantaneously to zero, but a small fraction η of the original response persisted for a while. This remaining effect slowly diminished due to thermal relaxation (of cages), when the sample was kept at the same elevated temperature. It can be frozen in by cooling to ambient temperature.

The fraction $\eta \equiv r_{\text{field off}}/r_{\text{field on}}$ can be considered as the efficiency of the freezing-in of polar order. The maximum value of η that could be attained in the test polymer was only about 0.4–0.5, which is smaller than normally found in the DANS polymer (0.6–0.7). See e.g. Figure 5. To reach these values more rigorous poling was necessary in the test polymer with $T_g = 175$°C (15 min at 180°C) than in the DANS polymer with $T_g = 140$°C (1 min at 140°C). The ultimate value of the EO coefficient is significantly smaller in the test polymer than in the DANS polymer (factor 2–3). These observations indicate more hindered rotatability in the test polymer than in the DANS polymer.

4.2.2. Relaxation

Relaxation experiments have been performed in two batches of the test polymer at several constant temperatures in the range from 80°C to 175°C. The decay of the EO coefficient r_{13} was measured with a FP interferometer and fitted with a single-exponential expression of time. Relaxation frequencies $\alpha(T)$ obtained at different temperatures are shown in the Arrhenius plot of Figure 6, for each of the two batches separately. In one batch, too few data points are available to allow a reliable construction of the Arrhenius line. In the other one, studied at many more temperatures, an activation energy A was found to be 155 kJ/mol and a pre-exponential factor given by $\ln[\alpha(\infty)] = 43$ (α in reciprocal hours). The experimental points of the two batches all overlap, so the difference is probably not significant. The activation energy of 155 kJ/mol is significantly smaller than the corresponding values measured in the DANS polymer with $T_g = 140$°C, which all are in the vicinity of 300 kJ/mol (Section 4.1.5).

Possibly, the lower activation energy of the $T_g = 175$°C test polymer and its evidently lower polability (preceding Subsection) are related. A more hindered polability is probably accompanied by a more hindered physical ageing process (shirinking of free volume). Since the difference between the non-equilibrium and the equilibrium value of the specific volume (free volume) increases on cooling to lower temperatures, the influence of the thermal history at high temperatures also increases on cooling to lower temperatures. In terms of the effective temperature concept of Rusch and Beck,[21,22,16] the difference between effective temperature and actual temperature becomes larger at lower (actual) temperatures. As a result, the measured activation energies in non-equilibrium polymers are too small. This effect is more pronounced, if physical ageing is more hindered, and still has a longer way to go during the EO relaxation measurements.

For temperatures above 100°C the test polymer with the higher T_g is more stable (lower α) than the polymer with $T_g = 140$°C. However, the two Arrhenius lines in Figure 6 approach each other at lower temperatures. At about 100°C, both polymers are equally stable. The straight Arrhenius lines obtained from least-squares fits cross each other at about 90°C, but whether the actual (curved?) lines do indeed cross remains to be

investigated. Recent experiments in this region, performed in both polymers at 80°C, do not indicate such a crossing. Instead, the data points of both polymers coincide and are above the corresponding straight lines in Figure 6, indicating that the real Arrhenius lines are curved lines with a smaller slope at lower temperatures.

5. SUMMARY

Test samples of NLO polymers are very suitable for fundamental studies of poling and relaxation. The poling behavior of a DANS polymer with $T_g = 140°C$ follows the predictions of the isotropic poling model for fields strengths up to 50–80 V/μm, as far as the ratio of the EO coefficients is concerned ($r_{33}/r_{13} = 3$), and linearity of the EO coefficients in the poling field strength. The magnitude of the experimental coefficients is significantly smaller than the theoretical predictions. Above 50–80 V/μm we do see indications of a superlinear dependence of r_{33} as a function of the poling field strength.

Only a fraction η of the field induced polar order can be frozen in. Fraction $(1 - \eta)$ is lost at the moment when the poling field is switched off. The influence of annealing on relaxation has been investigated. Annealing suppresses initial fast relaxation.

The poling and relaxation behavior of a new test polymer with a higher T_g (175°C) has been investigated and compared with the $T_g = 140°C$ polymer. The polymer with the higher T_g is more stable for temperatures above 100°C. The relaxation behavior of both polymers below 100°C is still being investigated. The induced EO coefficients are significantly smaller in the test polymer with the higher T_g.

Acknowledgments

The authors wish to thank Dr. C. T. J. Wreesmann, Dr. F. C. J. M. van Veggel and B. H. M. Hams for the organic syntheses, Dr. L. W. Jenneskens and Dr. J. W. Hofstraat for the DSC measurements and Dr. G. C. Dubbeldam and A. Anema for the refractive index measurements.

References

1. D. J. Williams, *ACS Symposium Series 233,* (Am. Chem. Soc., Washington, D. C., 1983).
2. C. P. J. M. van der Vorst, W. H. G. Horsthuis, and G. R. Möhlmann, *Polymers for Lightwave and Integrated Optics: Technology and Applications,* Ed. L. A. Hornak (Marcel Dekker, Inc., New York, 1992), Chap. 14, p. 365.
3. G. R. Möhlmann and van der C. P. J. M. Vorst, *Side Chain Liquid Crystal Polymers,* Ed. C. B. McArdle (Blackie and Son Ltd., London, 1989), Chap. 12, p. 330.
4. G. R. Möhlmann, W. H. G. Horsthuis, J. W. Mertens, M. B. J. Diemeer, F. M. M. Suyten, B. Hendriksen, C. Duchet, P. Fabre, C. Brot, J. M. Copeland, J. R. Mellor, E. van Tomme, P. van Daele, and R. Baets, *SPIE Proceedings,* **1560,** 426 (1991).
5. W. H. G. Horsthuis, F. C. J. M. van Veggel, B. H. M. Hams, C. P. J. M. van der Vorst, J. L. Heideman, H. W. Mertens, M. van Rheede, and G. R. Möhlmann, *SPIE Proceedings,* **1775,** in press.
6. D. G. Girton, G. F. Kwiatkowsky, G. F. Lipscomb, and R. Lytel, *Appl. Phys. Lett.,* **58,** 1730 (1991).
7. G. F. Lipscomb, R. S. Lytel, A. J. Thicknor, T. E. van Eck, S. L. Kwiatkowski, and D. G. Girton, *SPIE Proceedings,* **1337,** 23 (1990).
8. C. P. J. M. van der Vorst and R. A. Huijts, *SPIE Proceedings,* **1126,** 6 (1989).
9. C. P. J. M. van der Vorst and C. J. M. van Weerdenburg, *SPIE Proceedings,* **1337,** 246 (1990).
10. C. A. Eldering, A. Knoesen, and S. T. Kowel, *SPIE Proceedings,* **1337,** 348 (1990).
11. M. Sigelle and R. Hierle, *J. Appl. Phys.,* **52,** 4199 (1981).

12. G. R. Meredith, J. G. van Dusen, and D. J. Williams, *Macromolecules*, **15,** 1385 (1982).
13. G. R. Meredith, J. G. van Dusen, and D. J. Williams, *ACS Symposium Series 233*, (Am. Chem. Soc., Washington, D. C., 1983), Chap. 5, p. 109.
14. C. P. J. M. van der Vorst and S. J. Picken, *J. Opt. Soc. Am.*, **B7,** 320 (1990).
15. J. B. Stamatoff, *Technical Digest Series*, Vol. 5, contribution MA2 (1990).
16. H. T. Man and H. N. Yoon, *Adv. Mater.*, **4,** 159 (1992).
17. S. C. Lee, A. Kidoguchi, T. Watanabe, H. Yamamoto, T. Hosomi, and S. Miyata, *Polymer Journal*, **23,** 1209 (1991).
18. W. Köhler, D. R. Robello, P. T. Dao, C. S. Willand, and D. J. Williams, *J. Chem. Phys.*, **93,** 9157 (1990).
19. C. P. J. M. van der Vorst and M. van Rheede, *SPIE Proceeding*, **1775** in press.
20. J. F. Valley, private communication 1990; J. F. Valley and J. W. Wu, *SPIE Proceedings*, **1337,** 226 (1990).
21. K. C. Rusch, *J. Macromol. Sci. Phys.*, **B2,** 179 (1968).
22. K. C. Rusch and R. H. Beck, *J. Macromol. Sci. Phys.*, **B3,** 365 (1969).